International Journal of Engineering & Technology, 7 (4.30) (2018) 126-130

International Journal of Engineering & Technology

Website: www.sciencepubco.com/index.php/IJET

Research paper

Optical Temperature Sensor based on Sagnac Interferometer

Mohd Azwadi Omar[1], Noran Azizan Cholan[1,2]*, Aminuddin Mohd[1], Mirsa Nurfarhan Mohd Azhan[1], Rahmat Talib[1], Nor Hafizah Ngajikin[1]

[1]Facultyof Electrical and Electronics Engineering, Universiti Tun Hussein Onn Malaysia, 86400 Parit Raja, Batu Pahat, Johor, Malaysia
[2]Research Center for Applied Electromagnetics, Universiti Tun Hussein Onn Malaysia, 86400 Parit Raja, Batu Pahat, Johor, Malaysia
**Corresponding author E-mail:noran@uthm.edu.my*

Abstract

Optical temperature sensors gain interest from the community recently due to their immunity to electromagnetic interference and ruggedness against chemical and mechanical disturbances as opposed to the conventional temperature sensors such as thermocouples and resistance temperature detectors. Optical temperature sensors come with many varieties and Sagnac interferometer is one of them. In this work, an all-fiber temperature sensor is proposed and experimentally demonstrated. The proposed optical temperature utilizes Sagnac interferometer as the temperature head. The underlying mechanism for this sensor is based on the temperature dependence of a polarization maintaining fiber (PMF) in the Sagnac interferometer. The PMF birefringence which is influenced by temperature affects the phase difference of two incoming lights that enter the Sagnac interferometer and this contributes to the shifting of the transmission spectrum. The input light for the sensor characterization is provided by a custom-made amplified spontaneous emission source which comprises of a tunable laser source, a 980 nm laser diode pump, a wavelength division multiplexing coupler and a 10 m long erbium-doped fiber. Experimental results indicate that the temperature does affect the PMF characteristic. As the temperature increases from 30°C to 45°C, the wavelength dip reduced from 1553.8 nm to 1536.78nm. This proposed optical temperature sensor has a sensitivity of-1.0345 nm/°C. The development of this optical temperature sensor is promising especially for the measurement in the harsh environment.

Keywords:*Fiber Optics; Optical Sensor; Sagnac Interferometer; Sensor Sensitivity; Temperature.*

1. Introduction

Temperature monitoring is required in many applications such as automated production plants and high performance processors. Therefore, on-site temperature measurement is of significant importance in order to ensure smooth operation of a system. Conventional methods for temperature measurement utilize thermocouples and resistance temperature detectors (RTDs). However, they are prone to disturbances and this is especially true in hostile environment that includes tunnels, nuclear reactors and aerospace systems to name a few. In such systems, electromagnetic, chemical and mechanical disturbances come into play, causing the performance of temperature measurement to be unsatisfactory. As such, fiber optical sensors become a better alternative than thermocouples and RTDs since optical fibers are immune to electromagnetic interference and more rugged against chemical and mechanical disturbances. Different configurations of optical sensors for temperature measurement have been demonstrated such as core-mismatch fiber structure [1], Fabry-Pérot interferometer (FPI) [2], micro-cavity structure [3] and photonic crystal fiber (PCF) [4]. In separate advances, techniques of multimode interference [5] and surface plasmon resonance [6], [7] have also been utilized for the development of optical temperature sensors.
In general, optical fiber sensor can be categorized intowave-length modulated sensors, intensity modulated sensors and interferometric sensors. The wavelength modulated sensors that work based on grating concept such as Fiber Bragg Grating (FBG) offers a wide dynamic range with high sensitivity [8]-[10]. However, this type of sensor is complex in its fabrication. On the other hand, intensity modulated sensor has low fabrication complexity due to its simplest configuration, but has drawback in its sensitivity performance and can be easily influenced by intensity fluctuation of the laser source [11]-[13]. As for Mach-Zhender, Sagnac and Fabry-Perot interferometric sensors, the sensors have comparable sensitivity to wavelength modulated sensor with easier fabrication process and more stable compared to intensity modulated sensor [14]-[19].
In this work, a Sagnac interferometer is incorporated for the temperature measurement. The Sagnac interferometer consists of a 3-dB coupler, a polarization controller (PC) and a polarization maintaining fiber (PMF) which acts as a temperature sensor head. As the temperature of the PMF increases from 30 °C to 45 °C, the wavelength dip shifts from 1553.8 nm to 1536.78nm. Based on a linear fitting, the proposed optical temperature sensor has a sensitivity of -1.0345 nm/°C.

2. Experimental Setup

Figure 1 shows the experimental setup of the Sagnac interferometer based-optical temperature sensor. The Sagnac interferometer consists of a 3-dB coupler, a PC and a 2.2 cm PMF which acts as a temperature sensor head. The PMF is placed in a temperature chamber (i.e Venticell 55) for experiencing different values of temperature. The input light in this experiment is provided by a custom-made amplified spontaneous emission (ASE) source

which comprises of a tunable laser source (TLS), a 980 nm laser diode pump, a WDM coupler and a 10 m erbium-doped fiber (EDF). When the TLS is turned off and the laser diode is turned on, that means only the 980 nm pump light propagates through the EDF. Consequently, spontaneous emission dominates over stimulated emission in the EDF due to the disappearance of signal light, generating ASE noise at the output of the EDF as a result [20]. The spectrum of the output light sensor is captured by an optical spectrum analyzer (OSA) to measure the wavelength shifting and transmission for different temperature. The OSA has a resolution of 0.02 nm. The real experimental setupof the Sagnac interferometer based-optical temperature sensor is illustrated in Figure 2.

The mechanism for the Sagnac interferometer as temperature sensor is illustrated in Figure 3. The explanation is as follows; the input light of ASE is split into two propagating beams when it passes a polarization-insensitive 3dB coupler. The two propagating beams travel in two paths; the first beam travels in the clockwise (CW) direction and the second beam travels in the counter clockwise (CCW) direction. Both incident beams pass through the PMF and PC before they recombine in the 3-dB coupler, forming interference spectrum at the output of the Sagnac interferometer. The transmission spectrum has periodic characteristic, which can be expressed as [21]

$$T = (1-\cos\varphi)/2 \tag{1}$$

where, φ is the phase difference between the CW and CCW beam. The phase difference, φ, is in turn defined by

$$\varphi = 2\pi BL/\lambda \tag{2}$$

where, B is the PMF birefringence, L is the PMF length and λ is the input light wavelength. As the temperature of the PMF changes, which can be varied through the temperature chamber, the birefringence of the PMF is affected as well. This leads to the change of the phase difference between the CW and CCW beam. The new phase difference, φ', resulting from the birefringence change, ΔB, is formulated as [22]

$$\varphi' = 2\pi(B+\Delta B)L/\lambda \tag{3}$$

Correspondingly, the change of the phase difference, $\Delta\varphi$, is denoted by

$$\Delta\varphi = \varphi' - \varphi = 2\pi\Delta BL/\lambda \tag{4}$$

The equation (4) indicates that the PMF birefringence which is influenced by temperature, affects the phase difference, thus contributing to the shifting of the transmission spectrum. This temperature sensitivity of the spectrum shifting is utilized as underlying mechanism for optical temperature sensor.

In this work, the measurement is carried out by placing the temperature sensing fiber in the Venticell 55 laboratory oven that has working temperature ranging from +10 ^{0}C to 250 ^{0}C. The temperature sensor based on Sagnac interferometer is a non-contact temperature sensor that operates on some form of radiative heat transfer measurement. Heat radiated from oven heating element is detected by the sensing fiber, hence influencing the phase difference of the interferometer. Figure 4 shows the image of the Venticell 55 laboratory oven and Figure 5 illustrates the location of the sensing fiber probe. The sensing fiber is located at the middle of the oven by assuming the heat is uniformly distributed at that location.

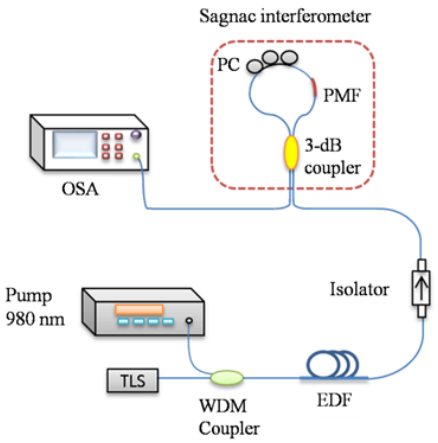

Fig. 1: Experimental setup of optical temperature sensor based on Sagnac interferometer.

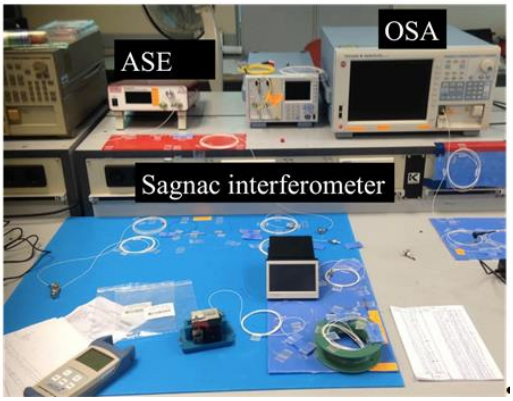

Fig. 2: Real experimental setup of optical temperature sensor based on Sagnac interferometer.

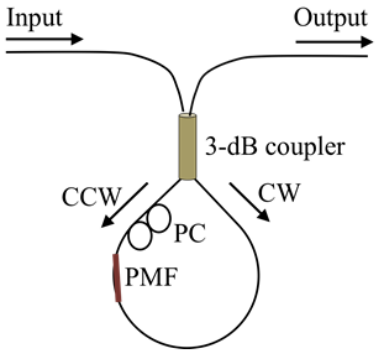

Fig. 3: Mechanism of Sagnac interferometer as superposition of clockwise (CW) and counter-clockwise (CCW) light.

Fig. 4: Venticell 55 laboratory oven

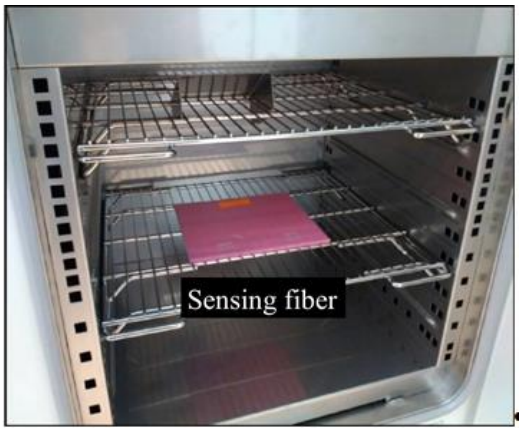

Fig. 5: Sensing fiber location in Venticell 55 laboratory oven

3. Results and Discussion

The generation of the ASE signal as the input source for the temperature sensor head is firstly investigated. The experimental setup for the generation of the ASE signal is illustrated in Fig. 6. The generation of ASE signal is possible when the laser diode is turned on and no input signal is present. In this case, only pump light at 980 nm wavelength propagates into the EDF. Consequently, erbium ions in the EDF are excited in the upper state and due to the absence of the input signal, excited erbium ions fall down to the lower state through spontaneous emission process. Spectrum of the signal emitted from the spontaneous emission process span over a wide range and for this reason, the ASE signal cover a C band region from 1530 nm to 1565 nm. The spectrum of the ASE signal is shown in Fig. 7.

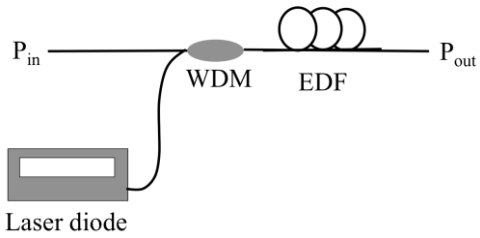

Fig. 6: Experimental setup of ASE generation.

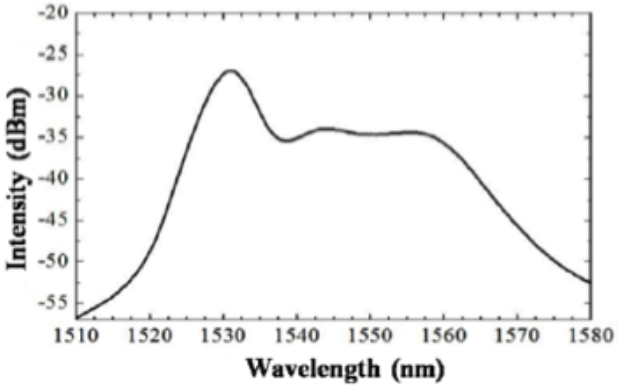

Fig. 7: Spectrum of ASE signal.

In the case where both signal and pump present in the EDF, the device acts as an optical amplifier. Figure 8 shows the spectrum of the input signal at the wavelength of 1564.5 nm. When both input signal and pump propagate in the EDF, stimulated emission process takes place. As the input signal passes through the EDF, it forces the excited erbium ions to fall down to the lower level. Due to energy conversion, new light is emitted and this will add up the existing input light. As a result, the input light is amplified. The spectrum of the amplified light illustrated in Figure 9 and it is evident that the amplified light sits on top of the amplifier noise. For this reason, optical amplifier adds up noise to the input signal.

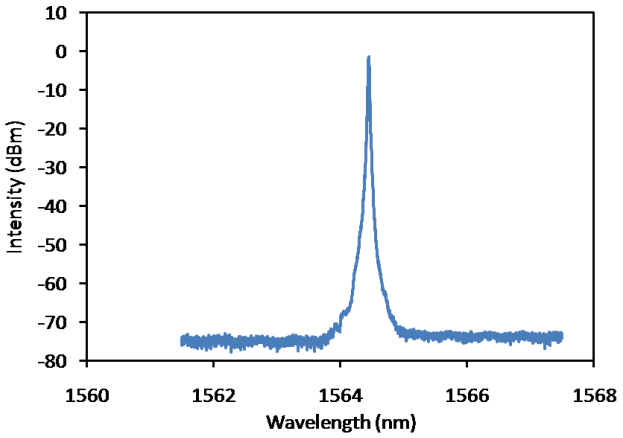

Fig. 8: Spectrum of input signal.

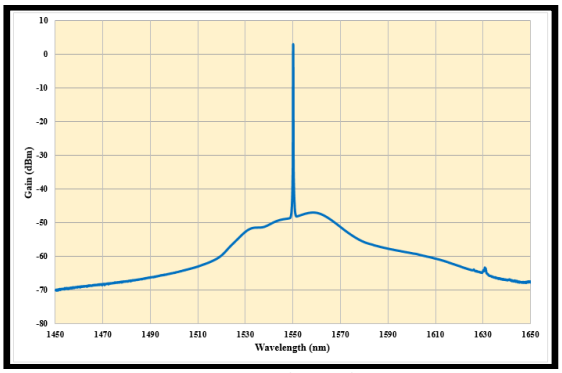

Fig. 9: Spectrum of amplified signal.

The characteristic of the input ASE signal is then investigated further. The spectrum of the ASE signal after the 10 m EDF is observed through OSA as shown in Fig. 10. It is evident that as the input current to the laser diode pump increases from 100 mA to 500 mA, the intensity of the ASE signal increases correspondingly. This is a consequence of a higher amount of excited erbium ions when the input current increases. The larger number of exited erbium ions prompts for a more dominance of spontaneous emission process in the EDF [23],[24]. As a result, the ASE intensity is enhanced as more current is pumped into the 980 nm laser diode. Another point to note in Fig. 2 is that the emission of the ASE covers over the C-band region which falls from 1530 nm to 1565 nm. This suggests that the length of ASE of 10 m is optimized for the amplification in the C-band region.

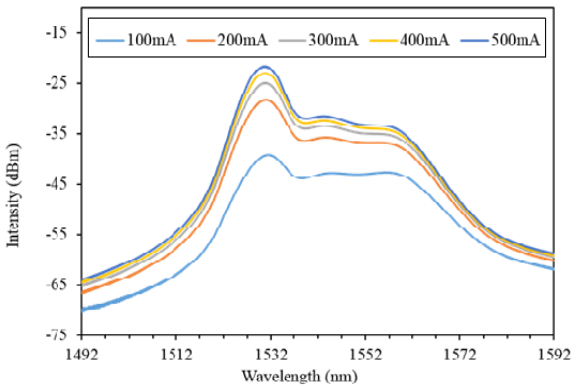

Fig. 10: Behavior of ASE spectrum as pump current increases .

The impact of temperature on the Sagnac interferometer or specifically PMF, which acts as the sensorhead is then examined. Fig. 11 shows the behaviour of the transmission spectra with different temperatures. Based on Fig. 11, there exists a wavelength dip for each spectrum. The wavelength dip results from the interference effect of the CW and CCW beams in the 3-dB coupler. As the temperature changes from 30°C to 45 °C, the wavelength dip shifts to the lower wavelength. The reason for this behaviour is that a change of temperature induces a change of birefringence in the PMF. As a result, the phase difference between the CW and CCW beams changes accordingly, leading to a change of the wavelength dip of the transmission spectrum. In essence, temperature parameter does affect the transmission spectra of Sagnac interferometer.

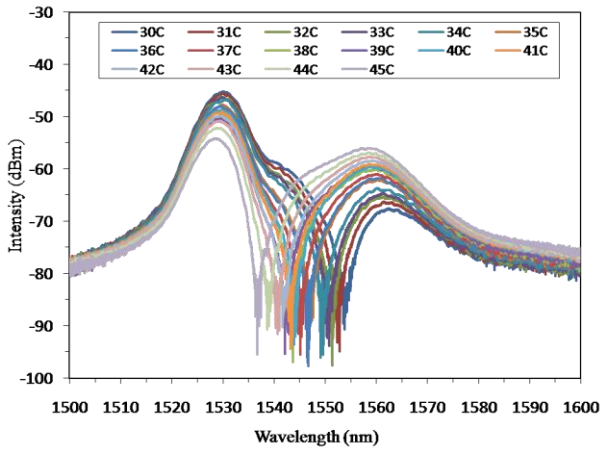

Fig. 11: Transmission spectra of Sagnac interferometer.

The sensitivity of the optical temperature sensor is then explored. Figure 12 shows the behavior of the wavelength dip as a function of temperature. As the temperature changes from 30 °C to 45 °C, the wavelength dip shifts from 1553.8 nm to 1536.78nm. Based on Fig. 12, the wavelength dip has a linear relationship with the temperature. The linear fitting has a R2 of 0.967 and the slope of -1.0345 nm/°C which also represents the sensitivity of the optical temperature sensor.

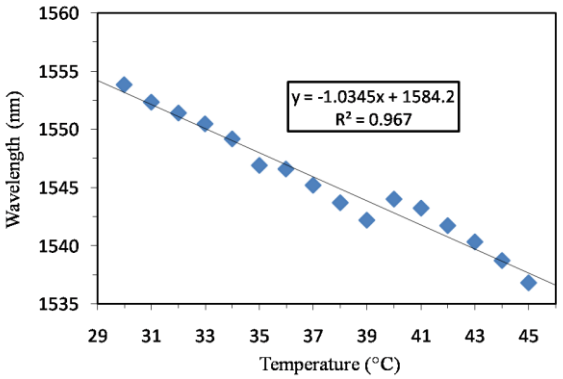

Fig. 12: Wavelength dip as function of temperature.

4. Conclusion

In summary, an all-fiber temperature sensor has been proposed and experimentally demonstrated. The configuration of the temperature sensor is based on Sagnac interferometer which also acts as the temperature sensor head. The input light for the sensor characterization is provided by a custom-made amplified spontaneous emission source which comprises of a tunable laser source, a 980 nm laser diode pump, a wavelength division multiplexing coupler and a 10 m long erbium-doped fiber.Due to birefringence change in the PMF, the wavelength dip reduces from 1553.8 nm to 1536.78nm as the temperature increases from 30 °C to 45 °C. The proposed optical temperature sensor has a sensitivity of -1.0345 nm/°C. Compared to conventional temperature sensors, the development of this optical temperature sensor is promising due to their immunity to electromagnetic interference and ruggedness against chemical and mechanical disturbances.

Acknowledgement

This work was supported in part by the Universiti Tun Hussein Onn Malaysia (UTHM) under TIER 1 Research Grant Vot H162 and Post-Graduate Research Grant(GPPS) Vot U591.

References

[1] Wang F, Zhu H, Li Y, Zhao H, Wang X & Liu Y (2016), Comparative study on a core-offset fiber temperature sensor between the Faraday rotation mirror structure and the double coupling structure, *Optics Communication*, 367, 286–291.

[2] Tafulo PAR, Jorge PAS, Santos JL, Araújo FM &Frazão O (2012), Intrinsic Fabry–Pérot cavity sensor based on etched multimode graded index fiber for strain and temperature measurement, *IEEE Sensors Journal*, 12, 8–12.

[3] Hernández-Romano I et al. (2016), Optical fiber temperature sensor based on a microcavity with polymer overlay, *Optics Express*, 24, 5654–5661.

[4] Wu C, Fu HY, Qureshi KK, Guan BO &Tam HY (2011), High pressure and high-temperature characteristics of a Fabry–Pérot interferometer based on photonic crystal fiber, *Optics Letter*, 36, 412–414.

[5] Tong Z, Luan P, Cao PY, Zhang W &Su J (2016), Dual-parameter optical fiber sensor based on concatenated down-taper and multimode fiber, *Optics Communication*, 358, 77–81.

[6] Luan N, Ding C &Yao J (2016), A refractive index and temperature sensor based on surface plasmon resonance in an exposed-core microstructured optical fiber, *IEEE Photonics Journal*, 8, 4801608.

[7] Liu Cet al. (2016), A highly temperature-sensitive photonic crystal fiber based on surface plasmon resonance, *Optics Communication*, 359, 378–382.

[8] Zhu Y, Shum P, Lu C, Lacquet MB, Swart PL, Chtcerbakov AA &Spammer SJ (2003), Temperature insensitive measurements of static displacements using a fiber Bragg grating,*Optics Express*, 11, 1918-1924.

[9] Jiang SJ, Wang J, Sui QM &Cao YQ (2015) A novel wide measuring range FBG displacement sensor with variable measurement precision based on helical bevel gear, *Optoelectronics Letter*, 11, 81-83.

[10] Li JC, Neumann H &Ramalingam R (2015), Design, fabrication and testing of fiber Bragg grating sensors for cryogenic long range displacement measurement, *Cyrogenics*, 68, 36-43.

[11] Shimamoto A &Tanaka K (1995), Optical fiber bundle displacement sensor using an ac-modulated light source with subnanometer resolution and low thermal drift, *Applied Optics*,34, 25, 5854-5860.

[12] Fujiwara E, Dos Santos MFM &Suzuki CK (2014), Flexible optical fiber bending transducer for application in gloved-based sensor, *IEEE Sensors Journal*, 14 (10), 3631-3636.

[13] Liu J, Hou Y, Jia P, Su S, Fang G, Liu W &Xiong J (2017), A wide-range displacement sensor based on plastic fiber macro bending coupling, *Sensors*, MDPI, 17, 196.

[14] Chen JP, Zhou J&Jia ZH (2013), High sensitivity displacement sensor based on a bent fiber Mach-Zhender interferometer, *IEEE Photonics Technology Letters*, 25 (23), 2354-2357.

[15] DashJN, Jha R, Villatoro J &Dass S (2015), Nano displacement sensor based on photonic crystal fiber modal interferomete, *Optics Letter*, 40(4), 467-470.

[16] Rong Q, Qiao X, Du Y, Feng D, Wang R, Ma Y, Sun H, Hu M &Feng Z (2013), In fiber quasi-Michelson interferometer with a core-cladding-mode fiber end-face mirror, *Applied Optics*, 52(7), 1441-1447.

[17] Ismail NI, Ngajikin NH, Zaman NFM, Awang M, Azmi AI, Malik NNNA & Kassim NM (2014), Resolution Improvement in Fabry-Perot Displacement Sensor Based on Fringe Counting Method, *Telkomnika*, 12(4), 811-818.

[18] Bai Y, Yan F, Liu S & Wen X (2016), All fiber Fabry-Perot interferometer for high sensitive micro displacement sensing, *Opt. Quantum Electron*, 48, 206.
[19] Lee BH, Kim YH, Park KS, Eom JB, Kim MJ, Rho BS & Choi HY (2012), Interferometric fiber optics sensors, *Sensors*, MDPI, 12, pp. 2467-2486.
[20] Cholan NA, Al-Mansoori MH, Noor ASM, Ismail A &Mahdi MA (2014), Self-seeded four-wave mixing cascades with low power consumption, *Journal of Optics (UK)*, 16, 105203.
[21] Liu Y et al. (2005), High-birefringence fiber loop mirrors and their applications as sensors, *Applied Optics*, 44, 2382–2390.
[22] Gong H, Chan CC, Chen L &Dong X (2010), Strain sensor realized by using low-birefringence photonic-crystal-fiber-based Sagnac loop, *IEEE Photonics Technology Letter*, 22, 1238–1240.
[23] Saleh S, Cholan NA, Sulaiman AH & Mahdi MA (2018), Stable multiwavelength erbium-doped random fiber laser, *IEEE Journal of Selected Topics in Quantum Electronics*, 24, 00902016.
[24] Al-Alimi AW, Cholan NA, Yaacob MH, Abas AF, Alresheedi MT, & Mahdi MA (2017), "Wide bandwidth and flat multiwavelength Brillouin-erbium fiber laser," *Opt. Express* 25(16), 19382–19390.